Single-crystal Electron Spin Resonance Spectra of Tris(diethyldithiocarbamato)oxomolybdenum(v) and Chlorobis(diethyldithiocarbamato)-oxomolybdenum(v) diluted in Isomorphous Host Lattices

By **Brendan Gahan, Nepal C. Howlander,** and **Frank E. Mabbs,*** Chemistry Department, University of Manchester, Manchester M13 9PL

Room-temperature single-crystal e.s.r. spectra are reported for $[MoO(S_2CNEt_2)_3]$ diluted in the corresponding niobium compound, and for $[MoOCl(S_2CNEt_2)_2]$ diluted in $[MoO_2(S_2CNEt_2)_2]$. The principal molecular parameters for $[MoO(S_2CNEt_2)_3]$ are $g_1 = 1.970 \pm 0.001$, $g_2 = 1.978 \pm 0.001$, $g_3 = 1.985 \pm 0.001$, $A_1 = 56.9 \pm 0.2 \times 10^{-4}$ cm^{-1}, $A_2 = 33.6 \pm 0.2 \times 10^{-4}$ cm^{-1}, and $A_3 = 27.1 \pm 0.2 \times 10^{-4}$ cm^{-1}, whilst those for $[MoOCl(S_2CNEt_2)_2]$ are $g_1 = 1.945 \pm 0.001$, $g_2 = 1.958 \pm 0.001$, $g_3 = 1.984 \pm 0.001$, $A_1(Mo) = 24.1 \pm 0.2 \times 10^{-4}$ cm^{-1}, $A_2(Mo) = 27.5 \pm 0.2 \times 10^{-4}$ cm^{-1}, $A_3(Mo) = 61.4 \pm 0.4 \times 10^{-4}$ cm^{-1}, $|A_1(Cl)| = 2.6 \pm 0.1 \times 10^{-4}$ cm^{-1}, $|A_2(Cl)| = 4.5 \pm 0.1 \times 10^{-4}$ cm^{-1}, and $|A_3(Cl)| = 12.6 \pm 0.1 \times 10^{-4}$ cm^{-1}. In both compounds the principal axis systems for the g and metal hyperfine tensors are non-coincident. The electronic absorption spectra and angular variation of the single-crystal g values have been interpreted in terms of a parameterised angular-overlap model.

THE presence of molybdenum as an essential element in the redox enzymes nitrate reductase, xanthine and aldehyde oxidase, and sulphite oxidase is now well established [1] and has led to considerable renewed interest in the chemistry of this element. The observation of e.s.r. signals attributable to the molybdenum centre in these enzymes has resulted in this technique being extensively used in their study. Thus, for example, the similarity of the e.s.r. parameters obtained from solutions of molybdenum(v) and certain sulphur-donor ligands with those reported for the enzymes has strongly implicated sulphur as at least one of the donor atoms present.[2,3] Unfortunately there are very few instances where the species in solution has subsequently been isolated and its detailed geometric and electronic properties studied. However recent X-ray absorption fine structure studies [4-6] on xanthine and sulphite oxidase do support the presence of sulphur in the Mo co-ordination sphere. This makes it very important to have information on the relationship between e.s.r. parameters and the nature of the molybdenum co-ordination sphere. In view of the scarcity of this type of data we are continuing our studies of molybdenum(v) species in the solid state using single-crystal e.s.r., and where possible electronic absorption spectra.[7-12] As part of this work we now report the results of such a study of $[MoO(S_2CNEt_2)_3]$ and $[MoOCl(S_2CNEt_2)_2]$ diluted in isostructural host lattices.

EXPERIMENTAL

Preparation.—The compound $[MoO(S_2CNEt_2)_3]$ was prepared by treating $MoOCl_3$ with anhydrous $Na[S_2CNEt_2]$ (mol ratio 1 : 3) in CH_2Cl_2 under N_2. Concentration of the solution under vacuum yielded a dark purple powder, which was filtered off, washed with dry hexane, and dried *in vacuo* (Found: C, 32.0; H, 5.3; Mo, 17.5; N, 7.3; S, 34.2. Calc. for $C_{15}H_{30}MoN_3OS_6$: C, 32.4; H, 5.4; Mo, 17.3; N, 7.6; S, 34.5%). Single crystals of the isomorphous $[NbO(S_2CNEt_2)_3]$ containing *ca.* 2% $[MoO(S_2CNEt_2)_3]$ were grown from chloroform solutions.

The compound $[MoOCl(S_2CNEt_2)_2]$ was prepared by treating $MoOCl_3$ with anhydrous $Na[S_2CNEt_2]$ (mol ratio 1 : 2) in CH_2Cl_2 under N_2. Rapid concentration of the solution under vacuum yielded a dark brown powder (Found: C,

TABLE 1

Angular variation of the g-value resonance (H/G) and the molybdenum hyperfine splittings (ΔH/G) for molybdenum-diluted $[NbO(S_2NCEt_2)_3]$, $\nu = 35.070$ GHz

	ab plane, *a* at θ = 0		*ac** plane, *c** at θ = 0		*bc** plane, *b* at θ = 0			
					Molecule 1		Molecule 2	
θ/°	H	ΔH	H	ΔH	H	ΔH	H	ΔH
0	12 631	27.7	12 661	27.7	12 718	60.0	12 718	60.0
15	12 637	33.0	12 650	28.8	12 723	59.6	12 708	54.0
30	12 652	39.5	12 639	30.7	12 719	57.6	12 693	48.6
45	12 673	51.2	12 630	32.2	12 705	53.0	12 679	41.4
60	12 694	57.0	12 627	31.7	12 692	46.8	12 668	33.4
75	12 710	59.8	12 628	29.2	12 678	38.5	12 664	28.6
90	12 716	60.5	12 636	27.7	12 665	27.5	12 665	27.5
105	12 710	59.3	12 647	27.2	12 665	29.2	12 680	39.2
120	12 694	57.5	12 658	27.0	12 669	34.5	12 694	48.8
135	12 673	51.5	12 668	27.1	12 680	41.5	12 707	55.0
150	12 651	39.7	12 671	27.2	12 693	47.6	12 720	58.0
165	12 636	34.0	12 670	27.5	12 707	53.8	12 723	59.8
180	12 631	27.7	12 661	27.9	12 718	60.0	12 718	60.0

27.0; H, 4.6; Cl, 8.0; Mo, 21.6; N, 6.3; S, 28.8. Calc. for $C_{10}H_{20}ClMoN_2OS_4$: C, 27.0; H, 4.5; Cl, 8.0; Mo, 21.6; N, 6.3; S, 29.0%). We have been unable to grow single crystals of the pure compound suitable for e.s.r. measurements, but single crystals of $[MoO_2(S_2CNEt_2)_2]$ containing suitable quantities of $[MoOCl(S_2CNEt_2)_2]$ (up to 20% based on chloride analysis) have been obtained.

Crystallographic Measurements.—*X*-Ray powder diffraction measurements showed that $[MoO(S_2CNEt_2)_3]$ was isomorphous with the niobium analogue.[13] Orientation of the diluted crystals using oscillation and Weissenberg *X*-ray techniques also confirmed that the unit-cell dimensions of molybdenum-diluted $[NbO(S_2CNEt_2)_3]$ were identical to those reported for the pure niobium compound. We therefore assume that the geometries of the molybdenum and niobium compounds are identical. The unit-cell parameters for the mixed system $[MoO_2(S_2CNEt_2)_2]$–$[MoOCl(S_2CNEt_2)_2]$ (80—20%) were slightly larger than those for pure $[MoO_2(S_2CNEt_2)_2]$ [14] [a = 17.46, b = 8.62, c = 13.81 Å, β = 124.75° compared with a = 17.383 9(14), b = 8.665 6(7), c = 13.590(12) Å, β = 124.66(1)°], but we assume that the diluent has not seriously distorted the host lattice.

Electron Spin Resonance Measurements.—These were taken at room temperature and *Q*-band frequencies on equipment previously described.[15] The crystallographic axes for each crystal used were located by standard *X*-ray techniques. The accuracy of alignment of the crystals in the e.s.r. spectrometer was checked by observing the internal consistency of the observed angular variation of the spectra. The results of these measurements are summarised in Tables 1 and 2.

Electronic Absorption Spectra.—These were obtained on solutions and on poly(dimethylsiloxane) mulls at room temperature, on equipment described previously.[16] The results are summarised in Table 3.

TABLE 2

Angular variation of the g-value fields (H/G), molybdenum hyperfine splittings (ΔH_{Mo}/G), and the chlorine superhyperfine splittings (ΔH_{Cl}/G) for single crystals of $[MoOCl(S_2CNEt_2)_2]$ diluted in $[MoO_2(S_2CNEt_2)_2]$, ν = 34.580 GHz

	ab plane, *a* at θ = 0						*bc** plane, *b* at θ = 0						*ac** plane, *a* at θ = 0		
	Molecule 1			Molecule 2			Molecule 1			Molecule 2					
θ/°	H	ΔH_{Mo}	ΔH_{Cl}	H	ΔH_{Mo}	ΔH_{Cl}	H	ΔH_{Mo}	ΔH_{Cl}	H	ΔH_{Mo}	ΔH_{Cl}	H	ΔH_{Mo}	ΔH_{Cl}
0	12 571	36.0	12.0	12 571	36.0	12.0	12 588	49.0	3.3	12 588	49.0	3.3	12 570	37.0	12.0
15	12 510	44.5	11.0	12 629	29.5	12.3	12 573	56.0	3.6	12 605	40.0	3.0	12 581	32.0	13.3
30	12 470	50.0	9.5	12 685	27.0	12.0	12 569	62.0	5.0	12 621	34.0	3.6	12 597	28.0	13.7
45	12 464	53.0	7.5	12 694	29.5	10.8	12 571	64.0	6.3	12 631	30.5	5.0	12 607	27.0	13.2
60	12 484	55.0	5.0	12 683	35.5	9.0	12 581	61.5	6.7	12 631	35.5	6.0	12 615	32.0	11.6
75	12 530	53.0	3.0	12 646	43.0	6.0	12 596	56.0	6.9	12 623	41.5	6.3	12 621	39.0	10.0
90	12 589	50.0	3.0	12 589	50.0	3.0	12 612	49.0	7.0	12 612	49.0	7.0	12 614	48.5	7.7
105	12 651	42.5	6.3	12 530	53.5	3.0	12 628	40.0	6.3	12 590	56.0	7.0	12 602	51.0	6.0
120	12 687	35.0	9.0	12 488	55.0	5.0	12 635	32.5	5.7	12 576	61.0	6.6	12 587	53.0	5.0
135	12 696	29.0	10.8	12 467	52.5	8.0	12 630	30.0	4.7	12 564	64.0	5.9	12 574	52.5	5.5
150	12 677	27.5	12.0	12 479	49.0	10.0	12 621	35.5	3.3	12 565	62.0	4.5	12 565	49.0	8.0
165	12 631	30.0	12.3	12 517	44.0	11.0	12 605	41.0	3.0	12 574	55.0	3.6	12 564	44.0	10.0
180	12 571	36.0	12.0	12 571	36.0	12.0	12 588	49.0	3.3	12 588	49.0	3.3	12 570	37.0	12.0

TABLE 3

Electronic absorption spectra of $[MoO(S_2CNEt_2)_3]$ and $[MoOCl(S_2CNEt_2)_2]$

	Absorption maxima/10^3 cm^{-1}	
Compound	Mull	Solution [a]
$[MoO(S_2CNEt_2)_3]$ [b]	7.62	7.65 (20)
	14.43 (sh)	14.30 (sh) (50)
	18.63	19.50 (696)
	24.30	26.90 (938)
$[MoOCl(S_2CNEt_2)_2]$	13.53 (sh)	*c*
	19.51	
	d	

[a] Absorption coefficients (ε/dm^3 mol^{-1} cm^{-1}) are given in parentheses. [b] Dichloroethane solution. [c] Solutions decompose in the spectrometer beam. [d] Continuously rising absorption above *ca.* 20.0 × 10^3 cm^{-1}.

RESULTS

Electron Spin Resonance Measurements.—Crystals of molybdenum-diluted $[NbO(S_2CNEt_2)_3]$ belong to the space group $P2_1/a$.[13] The single-crystal e.s.r. spectra consisted of a signal from only one type of molecule in the *ab* and *ac** crystallographic planes and a signal from each of two differently oriented molecules in the *bc** crystallographic plane. Well resolved molybdenum hyperfine splittings were observed for the signals at all orientations of the crystals. In general for a monoclinic system we would have expected to observe two magnetically distinct molecules in the *ab* plane. Presumably the orientations of the principal molecular g values of the two differently oriented molecules in this plane are indeed equivalent. Treatment of the data according to the methods of Schonland [17] and Lund and Vanngard [18] gives the principal molecular g and A values in Table 4.

The geometry of $[NbO(S_2CNEt_2)_3]$ approximates to a pentagonal bipyramid with the oxygen atom at one of the axial sites, the other six co-ordination sites being occupied by the sulphur atoms of the three bidentate dithiocarbamates, two of which lie approximately in the equatorial plane and the other spanning axial and equatorial sites. The equatorial sulphur atoms are not coplanar, nor are they coplanar with the metal atom which lies well above the best plane through the sulphur atoms with all O–Nb–S angles greater than 90°. Although the molecule has been described as a pentagonal bipyramid a close examination of the bond angles and bond distances indicates that the only approximate symmetry element is that of a mirror plane through niobium, the oxo-ligand, and one of the equatorial sulphurs. Thus, the symmetry is far from the idealised C_{5v} and only approximates to C_s. As we have found in a number of other molybdenum systems of low symmetry [8,10,12] the axes of the principal g and A tensors do not coincide with

each other, and neither do they necessarily lie along any metal–ligand directions, for example parallel to terminal MoO, see Tables 5 and 8. In order to facilitate the interpretation of the single-crystal e.s.r. data we have defined an axis system for the molecule as z parallel to Nb=O, y in the plane O=Nb–S(22) (atom numbering of ref. 13) and perpendicular to z, and x as the normal to this plane.

TABLE 4

Principal molecular g and A (10^{-4} cm^{-1}) values and their direction cosines with respect to the crystallographic axes for molybdenum-diluted $[NbO(S_2CNEt_2)_3]$

		Direction cosines					
		Alternative 1			Alternative 2		
	g values	a	b	c^*	a	b	c^*
g_1	1.970 ± 0.001	−0.0482	−0.9662	0.2531	−0.0556	0.9653	−0.2550
g_2	1.978 ± 0.001	−0.4075	0.2503	0.8782	0.4047	0.2553	0.8781
g_3	1.985 ± 0.001	0.9119	0.0608	0.4058	−0.9128	0.0544	0.4048
A_1	56.9 ± 0.2	−0.0087	−0.9981	−0.0619	0.0026	0.9981	0.0612
A_2	33.6 ± 0.2	−0.3248	0.0613	−0.9438	0.3282	0.0570	−0.9429
A_3	27.1 ± 0.2	0.9457	0.0118	−0.3247	−0.9446	0.0226	−0.3274

TABLE 5

Angles between the principal molecular g and A values and the chosen molecular x, y, and z axes for molybdenum-diluted $[NbO(S_2CNEt_2)_3]$

Molecular direction †	Direction cosines		
	a	b	c^*
x	−0.9210	0.2006	−0.3340
y	0.0714	0.9303	0.3598
z	0.3829	0.3076	−0.8711

	Angle					
	Alternative 1			Alternative 2		
Molecular value	x	y	z	x	y	z
g_1	103.5	144.2	122.4	70.7	36.6	60.2
g_2	82.4	58.7	57.6	127.9	54.4	122.1
g_3	164.4	74.5	89.2	44.2	82.5	133.3
A_1	99.9	162.4	104.9	79.8	18.1	75.2
A_2	51.2	107.8	44.2	88.6	106.2	15.3
A_3	139.5	92.2	49.6	10.3	99.5	94.3

† See text for definition of the molecular x, y, and z directions.

$[MoOCl(S_2CNEt_2)_2]$ *in* $[MoO_2(S_2CNEt_2)_2]$. The compound $[MoO_2(S_2CNEt_2)_2]$ crystallises in the monoclinic space group $C2/c$. The co-ordination about the molybdenum atom is that of a distorted octahedron with a *cis* dioxo-arrangement. Each molecule has a two-fold rotation axis through the molybdenum atom which bisects the O–Mo–O angle and is parallel to the b axis. In the mixed crystal we assume that the $[MoOCl(S_2CNEt_2)_2]$ molecules occupy the $[MoO_2(S_2CNEt_2)_2]$ sites with chloride *cis* to the oxo-group, since the X-ray powder diffraction patterns of the two compounds are similar and the unit-cell parameters of the mixed crystals do not differ greatly from those o $[MoO_2(S_2CNEt_2)_2]$. In addition, the angular variation of the e.s.r. spectrum of the mixed crystals is also consistent with $[MoOCl(S_2CNEt_2)_2]$ occupying precise sites which are related by a two-fold rotation about the b axis.

As expected for a magnetically dilute single crystal, e.s.r. signals corresponding to two magnetically distinct molecules were observed in the ab and bc^* planes, but only to one molecule in the ac^* plane. Hyperfine splittings due to the nuclear spin of ^{95,97}Mo ($I = \frac{5}{2}$) isotopes were observed at all orientations of the crystal. Each main signal ($I_{Mo} = 0$) and each molybdenum hyperfine line ($I_{Mo} = \frac{5}{2}$) were further split in the ab and ac^* planes into four lines due to interaction of the unpaired $4d^1$ electron on the metal with the nuclear spin of the chlorine atom ($I_{Cl} = \frac{3}{2}$). The chlorine superhyperfine splittings in the ab and ac^* planes were measured from the $I_{Mo} = 0$ signals. In the bc^* plane the chlorine superhyperfine splitting was not resolved, this splitting being estimated from the width of the $I_{Mo} = 0$ signal. These data were treated according to the methods of Schonland [17] and Lund and Vanngard.[18] The principal molecular g, A(Mo), and A(Cl) values and their directions with respect to the crystallographic axes are given in Table 6. Assuming that $[MoOCl(S_2CNEt_2)_2]$ has the same geometry as $[MoO_2(S_2CNEt_2)_2]$ with one of the oxygens replaced by a chloride ion, then the molecule contains no symmetry elements. Some support for the assumption of essentially the same geometry for these two compounds is provided by the recent X-ray crystal structures [19] of $[MoO_2$(8-mercaptoquinolinate)$_2]$ and $[MoOCl$(8-mercaptoquinolinate)$_2]$ where the *cis* O–Mo–Cl arrangement has been demonstrated.

TABLE 6

Principal molecular g, A(Mo) (10^{-4} cm^{-1}), and A(Cl) (10^{-4} cm^{-1}) values and their direction cosines with respect to the crystallographic axes for $[MoOCl(S_2CNEt_2)_2]$ diluted in $[MoO_2(S_2CNEt_2)_2]$

		Direction cosines					
		Alternative 1			Alternative 2		
Principal molecular values		a	b	c^*	a	b	c^*
g_1	1.945 ± 0.001	0.6573	−0.7397	0.1441	0.6330	−0.7022	0.3259
g_2	1.958 ± 0.001	−0.2499	−0.0335	0.9677	0.2692	−0.1951	−0.9431
g_3	1.984 ± 0.001	0.7110	0.6721	0.2069	0.7259	0.6847	0.0655
A_1(Mo)	24.1 ± 0.2	0.9075	−0.2613	−0.3289	0.9041	0.3422	−0.2561
A_2(Mo)	27.5 ± 0.2	−0.0547	0.7029	−0.7092	0.0411	−0.6661	−0.7447
A_3(Mo)	61.4 ± 0.4	−0.4165	−0.6616	−0.6236	0.4254	−0.6627	0.6163
$\|A_1$(Cl)$\|$	2.6 ± 0.1	0.3473	−0.8423	−0.4122	0.3614	0.8402	−0.4044
$\|A_2$(Cl)$\|$	4.5 ± 0.1	0.3438	0.5233	−0.7797	0.3227	−0.5213	−0.7858
$\|A_3$(Cl)$\|$	12.6 ± 0.1	−0.8724	−0.1291	−0.4714	0.8711	−0.1494	0.4679

In addition, the interbond angles between similar atomic positions differ very little between these latter two compounds, thus making the assumption of the same geometry for $[MoOCl(S_2CNEt_2)_2]$ and $[MoO_2(S_2CNEt_2)_2]$ seem reasonable. Again to facilitate subsequent discussion of the e.s.r. data we have defined a molecular axis system for $[MoOCl(S_2CNEt_2)_2]$ as z parallel to Mo–O(1)′, y in the plane O(1)″–Mo–O(1)′ and perpendicular to z [the labelling of the

TABLE 7

Angles between the principal molecular g and A(Mo) values and the chosen molecular x, y, and z axes for $[MoOCl(S_2CNEt_2)_2]$ diluted in $[MoO_2(S_2CNEt_2)_2]$

Molecular direction †	Direction cosines		
	a	b	c^*
x	0.0399	0.0000	−0.9992
y	0.5422	−0.8398	0.0262
z	−0.8380	−0.5443	−0.0335

Molecular value	Angle					
	Alternative 1			Alternative 2		
	x	y	z	x	y	z
g_1	96.8	11.1	98.8	107.5	19.7	99.2
g_2	167.6	94.7	78.7	17.6	73.4	95.0
g_3	100.3	100.0	165.6	92.1	100.4	169.5
A_1(Mo)	68.6	45.3	127.4	73.0	78.6	159.3
A_2(Mo)	45.1	129.7	108.2	41.8	55.8	69.3
A_3(Mo)	52.7	71.7	43.1	126.8	36.5	90.9

† See text for molecular x, y, and z directions.

atoms is that of ref. 14 and we have assumed replacement of O(1)′ by Cl], and x perpendicular to the O(1)′–Mo–O(1)′ plane. For the $[MoO(S_2CNEt_2)_3]$ system, we again find that the principal axes of the g and A(Mo) tensors do not coincide with each other or with any molecular directions; see Tables 7 and 8.

Although there are significant differences between the orientations of the molecular g and A(Mo) tensors in each of the above compounds, the closest correspondence is for the smallest g values to be nearest to the largest A(Mo) value and *vice versa*. It is difficult to make a choice between the alternative orientations of the g and A tensors in these molecules although it is tempting to select the set which gives the

TABLE 8

Angles (°) between the principal molecular g and A tensors determined experimentally for $[MoO(S_2CNEt_2)_3]$ and $[MoOCl(S_2CNEt_2)_2]$

	Alternative 1			Alternative 2		
	A_1	A_2	A_3	A_1	A_2	A_3
$[MoO(S_2CNEt_2)_3]$						
g_1	18.4	106.4	98.0	18.6	73.9	80.9
g_2	107.5	132.9	131.9	72.0	132.9	131.6
g_3	95.4	132.5	43.0	85.6	132.7	43.0
$[MoOCl(S_2CNEt_2)_2]$						
g_1	42.1	131.2	82.8	75.6	75.5	20.7
g_2	122.4	134.1	118.5	65.3	32.5	109.7
g_3	66.3	73.3	141.6	29.1	118.4	96.0

tensor axes closest to symmetry or pseudo-symmetry axes. On this basis alternative 1 for $[MoO(S_2CNEt_2)_3]$ is preferred since this is nearly a tilting of the principal axes in the yz plane. This would be the situation if the plane containing O–Mo–S(22) was a true mirror plane. On this basis the orientations of the principal molecular g values seem to be different in the two molecules in that in $[MoO(S_2CNEt_2)_3]$ the largest g value is not associated with the terminal MoO direction but is closest to one of the in-plane sulphur atoms, a situation resembling that found in $[MoOCl_3(SPPh_3)]$.[10] In contrast to this the largest g value for $[MoOCl(S_2CNEt_2)_2]$ *is* the one nearest to the terminal MoO direction, comparable with the situation in the high-symmetry $[MoOX_4]^-$, $[MoOX_4L]^-$, where X = Cl or Br and L = H_2O, MeOH, MeCN, or $P(NMe_2)_3O$, in which $g_{\parallel} > g_{\perp}$.[9,20] Certainly in systems of low molecular symmetry the association of g values with particular molecular directions cannot be undertaken with any confidence when only powder or frozen-glass spectra are available. The two compounds studied here also serve to indicate the caution with which one should treat e.s.r. data from uncharacterised materials. Firstly, the common assumption that only one or two sulphur atoms in the molybdenum co-ordination sphere is sufficient to cause at least one g value to be equal to or greater than 2.0 is not generally valid. Our results indicate that the type of co-ordinated sulphur atom and/or the geometry of the complex is probably very important. Secondly, our results illustrate the dangers of assigning co-ordination spheres and geometries to species based only on their e.s.r. parameters. Thus we find that the e.s.r. parameters for $[MoO(S_2CNEt_2)_3]$ and $[Mo(S_2CNEt_2)_4]^+$ are very nearly identical {$g_{iso.} = 1.980$, $A_{iso.} = 34.8 \times 10^{-6}$ cm^{-1}, $g_1 = 1.970$, $g_2 = 1.978$, $g_3 = 1.985$ for $[MoO(S_2CNEt_2)_3]$ and $g_{iso.} = 1.980$, $A_{iso.} = 34.2 \times 10^{-4}$ cm^{-1}, $g_1 = 1.973$, $g_2 = 1.979$, and $g_3 = 1.987$ for $[Mo(S_2CNEt_2)_4]^+$}. Indeed the similarity of $g_{iso.}$ and $A_{iso.}$ has been used to suggest that the claim of Larin *et al.*[21] to have identified $[MoO(S_2CNEt_2)_3]$ in solution may be incorrect on the grounds that ' *it is barely conceivable that* $[MoO(S_2CNEt_2)_3]$ *and* $[Mo(S_2CNEt_2)_4]^+$ *have the same g and A values, and that the species identified was really the latter*'.[1]

The problem of the interpretation of the values and orientations of the principal molecular g values in low-symmetry molybdenum(v) complexes has previously been discussed qualitatively.[8,10,12] At this level the form of the equations for g_{ij} and A_{ij} demonstrated that the origin of the shift of the principal axes of the g tensor from chosen molecular directions, and also the non-coincidence of the principal axes of the g and A tensors, is caused by mixing between the metal-based nding orbitals allowed by the low symmetry. The ated form of the equations however does not permit oraic solution of the extent of this d-orbital mixing directly from the experimental g values. In an attempt to overcome this problem we have chosen to calculate this mixing using the angular-overlap model and subsequently calculate the e.s.r. parameters from this model. This has been used with success to interpret the single-crystal magnetic susceptibilities of first-row transition series complexes.[22]

Our approach has been to use the known molecular geometry with respect to a chosen axis system and to treat the angular-overlap parameters e_σ, $e_{\pi x}$, and $e_{\pi y}$ for each ligand as empirically adjustable parameters. In this way the d-orbital energies and their associated wave functions can be readily calculated as outlined by Gerloch and Slade.[23] Using these d-orbital functions and energies the molecular g tensor was calculated using the perturbation method of Abragam and Pryce.[24] Diagonalisation of the g tensor then gave the principal molecular g values and their orientations with respect to the chosen axis system. The squares of these principal g values were then transformed into the crystallographic a, b, c^* axis system and the angular variation of the e.s.r. spectrum was calculated for

comparison with the experimental data. The method of approach has been to vary the angular-overlap parameters to fit as many features of the absorption spectrum as possible, and finally to vary the orbital reduction parameters, k_x, k_y, k_z and the metal spin–orbit coupling constant ξ_M until the best fits to the principal molecular g values and angular variation of the e.s.r. spectrum was obtained. The results of this process are discussed below for each individual compound.

Calculation for $[MoO(S_2CNEt_2)_3]$.—The electronic absorption spectrum of this compound up to 30 000 cm^{-1} consisted of four absorption bands, the first two of which (7 650 and 14 300 cm^{-1}) may be attributed to d–d transitions based on their extinction coefficients, see Table 3. Thus the first stage of the calculation was to vary the angular-overlap parameters for the oxygen and six sulphur-donor atoms (each sulphur atom was assumed to have identical angular-overlap parameters) until transitions corresponding to these two energies were predicted. It was found that to calculate these transition energies to within $\pm 2\,000$ cm^{-1} then the angular-overlap parameters had to fall in the following ranges: $e_\sigma(S) = 12\,000$—$16\,000$ cm^{-1}, $e_\pi(S) = \pm 1\,000$ cm^{-1}; $e_\sigma(O) = 20\,000$—$80\,000$ cm^{-1}, $e_\pi(O) = 9\,000$—$12\,000$ cm^{-1}, where the symbol in parentheses represents the type of donor atom. Within these ranges it was found that the assumption of $e_{\pi x}(S) = e_{\pi y}(S)$ resulted in a larger calculated separation between the first two transitions than that observed. Thus if one of them was calculated correctly the other was automatically incorrect. This situation was however rectified if $e_{\pi x}(S) \neq e_{\pi y}(S)$, when both transitions could be simultaneously calculated to within better than 1 000 cm^{-1}. The best results were obtained with $e_\pi(S)$ perpendicular to the S_2C moiety being negative and $e_\pi(S)$ in the plane of this group being positive, for examples see Table 9. Some examples of combinations of parameters which do not simultaneously fit both absorption bands are also included in Table 9. Although the magnitudes of the $e_\pi(S)$ parameters are small, suggesting only weak π interactions, their signs imply that the dithiocarbamato-ligand is acting as a π acceptor perpendicular to the S_2C moiety and as a π donor in the plane. A similar disparity of the e_π parameters has been reported for the oxygen-donor atom in the acetato-ligand.[25] The parameter $e_\pi(O)$ *ca.* 10 000 cm^{-1} indicates that the terminal oxo-group is acting as a strong π donor, which is compatible with the currently accepted view of the mode of bonding of this ligand. The magnitude of the $e_\sigma(O)$ is indeterminate over a wide range, since it has only a small effect on either the calculated energies of the first three transitions or on the e.s.r. parameters. It is interesting to note that the parameters which enable the energies of the first two transitions to be predicted correctly also predict a transition which coincides with the third band in the absorption spectrum. On these grounds we suggest that this band is attributable to a d–d transition despite its high extinction coefficient. An example of one of the calculated d-orbital energy diagrams and the composition of the wave functions is given in Figure 1. Although there is significant intermixing of the metal d orbitals, the major components give the d orbital ordering $d_{xz} < d_{yz} < d_{xy} < d_{x^2-y^2} < d_{z^2}$ (*cf.* for C_{5v} d_{xz}, $d_{yz} < d_{xy}$, $d_{x^2-y^2} < d_{z^2}$). Thus the first band in the absorption spectrum represents the splitting of the d_{xz} and d_{yz} orbitals caused by departures from C_{5v} symmetry whilst the second and third transitions represent the split components of the d_{xy}, $d_{x^2-y^2}$ doublet in C_{5v} symmetry.

The angular-overlap parameters which gave a satisfactory interpretation of the electronic absorption spectrum were used for the calculation of the molecular g values. This was done by varying the k's at fixed values of ξ_{Mo} until the calculated principal molecular g values and angular variation of the e.s.r. spectrum were in satisfactory agreement with the experimental data. One example of the comparison between calculated and experimental data is illustrated in Figure 1. Since the effects of varying ξ_{Mo} and

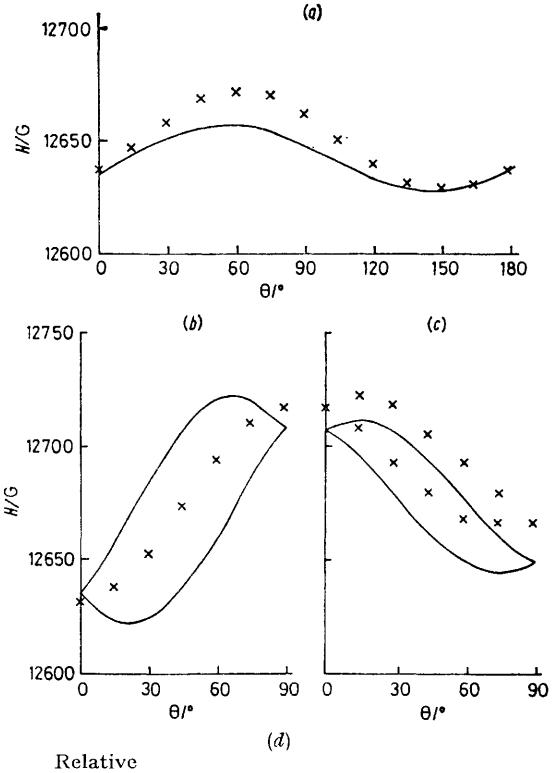

Relative d-orbital energy/10^3 cm^{-1}	Wave function
47.50	$-0.9753d_{z^2} + 0.2028d_{yz} - 0.0071d_{xz}$ $+0.0185d_{xy} + 0.0859d_{x^2-y^2}$
19.31	$0.0734d_{z^2} - 0.0607d_{yz} + 0.0394d_{xz}$ $-0.0583d_{xy} + 0.9930d_{x^2-y^2}$
14.99	$0.0170d_{z^2} + 0.1698d_{yz} - 0.3142d_{xz}$ $-0.9333d_{xy} - 0.0332d_{x^2-y^2}$
7.11	$-0\,2078d_{z^2} - 0.9570d_{yz} + 0.0419d_{xz}$ $-0.1900d_{xy} - 0.0560d_{x^2-y^2}$
0.00	$0.0044d_{z^2} + 0.1027d_{yz} + 0.9476d_{xz}$ $-0.2985d_{xy} - 0.0492d_{x^2-y^2}$

FIGURE 1 Comparison of the calculated (—) and experimental (×) angular variation of the e.s.r. spectrum of $[MoO(S_2CNEt_2)_3]$ for $e_\sigma(O) = 30.0 \times 10^3$, $e_\pi(O) = 10.0 \times 10^3$, $e_\sigma(S) = 13.0 \times 10^3$ cm^{-1}, $e_\pi(\perp S)/e_\pi(\parallel S) = -0.7/0.7$, $\xi_{Mo} = 630$ cm^{-1}, $k_x = 0.48$, $k_y = 0.50$, and $k_z = 0.36$. (*a*) ac^*, (*b*) ab, (*c*) bc^* planes, and (*d*) the calculated relative energies and wave functions of the d orbitals

k are not independent and an independent assessment of ξ_{Mo} is not possible, we have illustrated the calculation with the free-ion value appropriate to Mo^+.[26] Increasing ξ_{Mo} would simply require decreasing the values of k and *vice versa*. Once the electronic absorption spectrum has been satisfactorily predicted the values of k required to fit the e.s.r. data for this particular value of ξ_{Mo} fall in the ranges $k_x = 0.45$—0.50, $k_y = 0.48$—0.50, and $k_z = 0.30$—0.35. The calculation illustrated in Figure 1 gives good agreement between the angular variation in both the ac^* and bc^*

planes, the *maximum* difference between observed and calculated magnetic fields being 20 in *ca.* 12 650 G * (*i.e.* <0.2%). The agreement between calculated and experimental data is not quite as good in the *ab* plane. We cannot find a combination of parameters which make the e.s.r. behaviour of the two molecules identical in this plane. However the maximum difference between the calculated and observed data is still only 40 in *ca.* 12 650 G (*i.e.* ≈0.3%). Thus, overall this approach has enabled us to give a very satisfactory interpretation of both the absorption spectrum and the single-crystal e.s.r. spectrum of $[MoO(S_2CNEt_2)_3]$.

Calculation for $[MoOCl(S_2CNEt_2)_2]$.—We assume that $[MoOCl(S_2CNEt_2)_2]$ has the same geometry as $[MoO_2(S_2CNEt_2)_2]$, with one of the oxo-groups replaced by a chloro-ligand. The calculation was then approached as outlined above, with initial angular-overlap parameters for the oxo- and dithiocarbamato-ligands similar to those found satisfactory for $[MoO(S_2CNEt_2)_3]$, and those for the chloro-ligand from $[MoOCl_3\{OP(NMe_2)_3\}_2]$.[27] On this basis the *d–d* transitions were calculated to be *ca.* 8 000, 12 500, 28 000, and 44 000 cm^{-1}, see Table 10. The electronic absorption spectrum of a mull of $[MoOCl(S_2CNEt_2)_2]$ consisted of only two identifiable absorptions at 13 500 and 19 500 cm^{-1}, which are followed by a continuously increasing absorption. The initial calculation gave transition energies much lower than those observed. In order to correct this it was essential to increase $e_\pi(O)$ to *ca.* 20 000 cm^{-1}, which then predicted the first two transitions to within *ca.* 2 000 cm^{-1} of those observed, see Table 10. From this new starting point the energies of the first two transitions can be predicted to within 500 cm^{-1} of those observed by varying the other angular-overlap parameters. Increasing $e_\sigma(S)$ mainly increases the energy of the first transition as does increasing $e_\pi(S)$. On the other hand increasing $e_\sigma(O)$ increases the energy of the second transition and slightly decreases that of the first one. By suitably combining these effects the first two bands in the absorption spectrum were fitted with $e_\sigma(O) = 50.0 \times 10^3$, $e_\pi(O) = 20.0 \times 10^3$, $e_\sigma(S) = 18.0 \times 10^3$, $e_\pi(S)$ 2.0×10^3, $e_\sigma(Cl) = 13.0 \times 10^3$, and $e_\pi(Cl) = 1.0 \times 10^3$ cm^{-1}. Although separate angular-overlap parameters are quoted for the chloro- and dithiocarbamato-ligands these cannot be completely separately defined, since a change in the value of the parameters for one type of ligand can to some extent be compensated for by an appropriate change for the other ligands. However it is certain that $e_\pi(O)$ needs to be much larger in $[MoOCl(S_2CNEt_2)_2]$ than in $[MoO(S_2CNEt_2)_3]$, or $[MoOCl_3\{OP(NMe_2)_3\}]$,[27] and $[MoOCl_3(OPPh_3)_2]$,[27] implying considerably more π bonding from the terminal *oxo*-group. In addition $e_\sigma(S)$ is also greater for $[MoOCl(S_2CNEt_2)_2]$ compared with $[MoO(S_2CNEt_2)_3]$. These changes in parameters between the six- and seven-co-ordinate compounds are

* Throughout this paper: 1 G = 10^{-4} T.

TABLE 9

Angular-overlap parameters and calculated *d–d* transitions and principal molecular *g* values for $[MoO(S_2CNEt_2)_3]$. The *g* values are calculated for $\xi_{Mo} = 630$ cm^{-1}

Angular-overlap parameters/10^3 cm^{-1}					Calc. *d–d* transitions/10^3 cm^{-1}			
$e_\sigma(O)$	$e_\pi(O)$	$e_\sigma(S)$	$e_\pi(\perp S)$	$e_\pi(\parallel S)$				
50.0	10.0	13.0	−0.7	0.7	7.7	15.0	19.4	66.7
40.0	10.0	13.0	−0.7	0.7	7.5	15.0	19.3	57.0
30.0	10.0	13.0	−0.7	0.7	7.1	15.0	19.3	47.4
20.0	10.0	13.0	−0.7	0.7	6.5	15.0	19.2	38.0
30.0	10.0	13.0	1.0	1.0	4.0	11.3	14.2	41.8
30.0	10.0	13.0	0.0	0.0	4.6	12.4	15.4	45.1
30.0	10.0	13.0	−1.0	−1.0	5.1	13.4	16.7	48.3
30.0	10.0	14.0	−0.7	0.7	7.4	16.5	21.2	49.3
30.0	9.0	14.0	1.0	1.0	4.3	13.7	17.0	44.7
30.0	9.0	14.0	0.0	0.0	4.8	14.7	18.2	47.9
30.0	9.0	14.0	−1.0	−1.0	5.3	16.1	19.8	51.1
30.0	10.0	14.0	−1.0	0.0	5.9	16.3	20.7	50.3
30.0	10.0	14.0	1.0	0.0	2.8	11.6	13.9	43.7
30.0	10.0	14.0	−1.0	1.0	8.4	16.8	22.9	50.4

TABLE 10

Angular-overlap parameters and calculated *d–d* transition energies for $[MoOCl(S_2CNEt_2)_2]$

Angular-overlap parameters/10^3 cm^{-1}						Calc. *d–d* transition energies/10^3 cm^{-1}			
$e_\sigma(O)$	$e_\pi(O)$	$e_\sigma(S)$	$e_\pi(S)$	$e_\sigma(Cl)$	$e_\pi(Cl)$				
30.0	12.0	14.0	0.0	14.0	2.0	8.1	12.5	28.1	44.2
30.0	20.0	14.0	0.0	14.0	2.0	11.4	18.2	30.6	44.5
30.0	20.0	17.0	0.0	14.0	2.0	12.4	18.2	33.5	48.7
30.0	20.0	18.0	1.0	14.0	2.0	12.7	17.7	32.1	46.7
30.0	20.0	18.0	1.0	14.0	2.0	13.0	17.7	33.1	48.2
30.0	20.0	19.0	1.0	14.0	2.0	13.4	17.7	34.2	49.7
60.0	20.0	19.0	0.0	14.0	2.0	12.8	21.4	35.2	76.6
60.0	20.0	18.0	0.0	14.0	2.0	12.4	21.3	34.1	75.3
60.0	20.0	18.0	1.0	14.0	2.0	12.6	20.5	32.5	73.5
60.0	20.0	18.0	2.0	14.0	2.0	12.7	19.8	31.2	71.6
50.0	20.0	18.0	2.0	14.0	2.0	12.8	19.2	31.2	62.6
50.0	20.0	18.0	2.0	13.0	1.0	13.4	19.8	31.3	63.2
50.0	20.0	18.0	2.0	13.0	2.0	12.8	19.2	30.4	62.5

understandable at a qualitative level, since we would expect the metal–ligand distances to be shorter in the six-co-ordinate species.

The admixtures of *d*-orbital wave functions in the various energy levels are complicated, although the lowest level is comprised mainly of d_{xy}, whilst the highest is d_{z^2}. There is considerable intermixing of d_{yz} and d_{xz}, and also of d_{yz} and $d_{x^2-y^2}$. An example of the relative energy levels and associated wave functions is given in Figure 2.

The calculation of the e.s.r. behaviour based on these calculations has been generally less successful than for $[MoO(S_2CNEt_2)_3]$. We have not been able to find a combination of parameters which will simultaneously predict the principal molecular g_1 and g_2 values to better than *ca.* 0.5%. In particular g_1 is always too low whilst g_2 is too high. Although the resonance fields at the crystallographic axes can be calculated very close to those found experimentally the calculation results in too much difference between the two magnetically distinct molecules in the bc^* plane, and too little difference in the *ab* plane, see Figure 2, although the maximum error is only *ca.* 0.7% in terms of magnetic field. These discrepancies indicate that the model is not calculating the off-diagonal elements in the molecular *g* tensor with sufficient accuracy. It is worth pointing out however that this present application of the angular-overlap model represents an extremely severe test. Previously the model has been applied to the calculation of electronic absorption spectra, and of magnetic susceptibility measurements,[22,25] which provide no information on the angular variation of these properties for the differently oriented molecules in the unit cell. These latter measurements are equivalent to e.s.r. measurements on magnetically ' concentrated ' systems where the off-diagonal elements in the *ab* and bc^* planes average to zero. Under these circumstances we have previously demonstrated [27] that an excellent fit to the magnetically ' concentrated ' e.s.r. data can be obtained. Similarly if in $[MoOCl(S_2CNEt_2)_2]$ the arithmetic mean of the resonance positions in the *ab* and bc^* planes is compared with the corresponding calculated values, there is excellent agreement, see Figure 2(*f*).

We have now applied the angular-overlap model to the interpretation of the electronic absorption spectra and e.s.r. behaviour of four low-symmetry oxomolybdenum(v) complexes. The treatment seems to offer a reasonable method for interpreting the data on such systems, although discrepancies of up to *ca.* 1% may occur in some of the e.s.r. calculations.

Chlorine Superhyperfine Interaction.—The observation of chlorine superhyperfine splittings with magnitudes greater than those reported for the *cis* chloro-ligands in $[MoOCl_5]^{2-}$,[28] combined with the similar unit-cell dimensions of the diluted crystals, support the view that the chloro-ligand is *cis* to the *oxo*-group in $[MoOCl(S_2CNEt_2)_2]$. Chlorine superhyperfine splittings have previously been reported for toluene solutions of this compound by Larin *et al.*,[21] although these authors suggested that the chloro-group was probably *trans* to the oxo-group. These authors [21] found $A_{iso.}(Cl) = 3.2 \times 10^{-4}$ cm^{-1}. From our single-crystal data we obtain a value of 3.6×10^{-4} cm^{-1}, but only if we assume that $A_1(Cl)$ and $A_3(Cl)$ are positive and $A_2(Cl)$ is negative.

Because of the non-coincidence of the metal and ligand tensors, and the mixing of the *d*-orbital functions, a full analysis of the chlorine hyperfine tensor using the methods outlined by van Kemenade,[28] and by McGarvey [29] leads to complicated equations. These equations involve the molecular-orbital coefficients of all the metal-based antibonding molecular orbitals. In view of the large number of unknown parameters and the uncertainty as to the exact degree of metal *d*-orbital mixing, we at present only report an estimate of the ligand *s* and *p* orbital character in the ground-

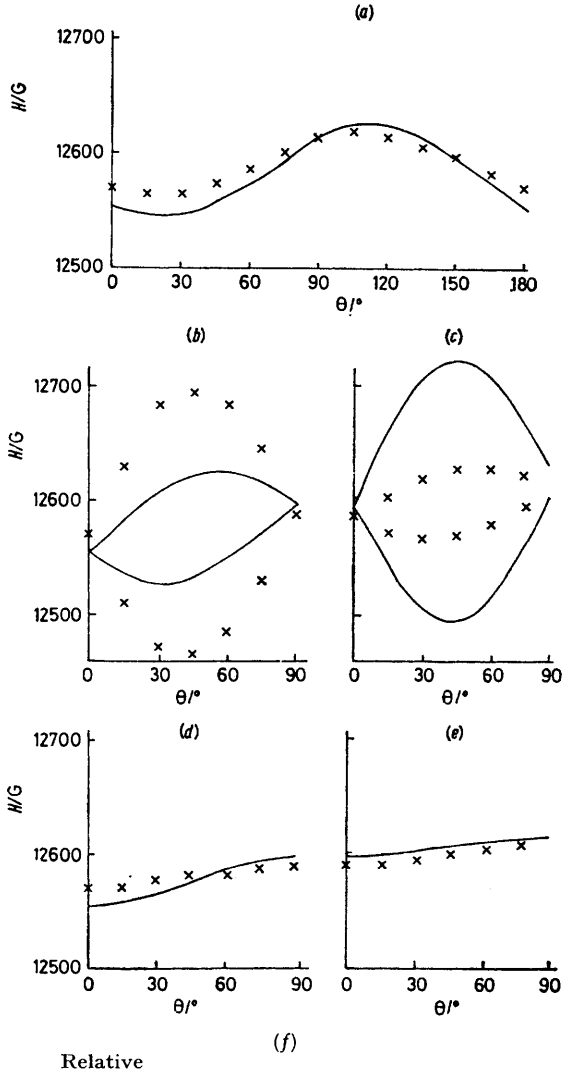

(*f*)

Relative *d*-orbital energy/10^3 cm^{-1}	Wave function
63.23	$-0.9479d_{z^2} - 0.1589d_{yz} - 0.2175d_{xz}$ $-0.1644d_{xy} + 0.0424d_{x^2-y^2}$
31.32	$0.0255d_{z^2} + 0.5690d_{yz} - 0.3650d_{xz}$ $-0.0092d_{xy} + 0.7364d_{x^2-y^2}$
19.78	$0.2917d_{z^2} - 0.5165d_{yz} - 0.7939d_{xz}$ $-0.1333d_{xy} - 0.0054d_{x^2-y^2}$
13.35	$0.0046d_{z^2} + 0.6063d_{yz} - 0.3311d_{xz}$ $-0.3421d_{xy} - 0.6370d_{x^2-y^2}$
0.00	$-0.1258d_{z^2} + 0.1286d_{yz} - 0.2820d_{xz}$ $+0.9155d_{xy} - 0.2236d_{x^2-y^2}$

FIGURE 2 Comparison of the calculated (—) and experimental (×) angular variation of the e.s.r. spectrum of $[MoOCl(S_2CNEt_2)_2]$ for $e_\sigma(O) = 50.0 \times 10^3$, $e_\pi(O) = 20.0 \times 10^3$, $e_\sigma(S) = 18.0 \times 10^3$, $e_\pi(S) = 2.0 \times 10^3$, $e_\sigma(Cl) = 13.0 \times 10^3$, $e_\pi(Cl) = 1.0 \times 10^3$, $\xi_{Mo} = 630$ cm^{-1}, $k_x = 0.83$, $k_y = 0.86$, and $k_z = 0.36$. (*a*) ac^*, (*b*) *ab*, (*c*) bc^* planes, (*d*) and (*e*) show the comparison between calculated and experimental arithmetic means of the resonance fields of the individual molecules in the *ab* and bc^* planes respectively, (*f*) the calculated relative energies and wave functions of the *d* orbitals

state molecular orbital using the approximate method outlined by Goodman and Raynor.[30] In this approach we have resolved the chlorine hyperfine tensor into an axis system parallel to x, y, z on the metal to give a_{xx}, a_{yy}, a_{zz}. After allowing for a dipolar contribution, using the point dipole approximation, and the isotropic contribution, a value of the ligand parameter $\alpha^2(p) = 0.10$ was obtained using the data in Table 4 ref. 30, and assuming Mo–Cl = 2.34 Å. The ligand isotropic hyperfine splitting parameter gives $\alpha^2(s) = 0.02$. These values indicate that the bonding is between the primarily d_{xy} ground state with a p orbital on the chloro-ligand.

We wish to thank the S.R.C. for support and one of us (N. C. H.) thanks the Commission for Commonwealth Scholarships in the U.K. for a research grant.

[0/422 *Received*, 17*th March*, 1980]

REFERENCES

[1] See for example, E. D. Stiefel, *Progr. Inorg. Chem.*, 1977, **22**, 14—25 and refs. therein.
[2] L. S. Meriwether, W. F. Narcliff, and W. G. Hodgson, *Nature*, 1966, **212**, 465.
[3] T. Huang and G. P. Haight, jun., *J. Amer. Chem. Soc.*, 1970, **92**, 2336; 1971, **93**, 611; *Chem. Comm.*, 1969, 985.
[4] T. D. Tullius, D. M. Kurtz, S. D. Conradson, and K. O. Hodgson, *J. Amer. Chem. Soc.*, 1979, **101**, 2776.
[5] S. P. Cramer, H. B. Gray, and K. V. Rajagopalan, *J. Amer. Chem. Soc.*, 1979, **101**, 2772.
[6] J. Bordas, R. C. Bray, C. D. Garner, S. Gutteridge, and S. S. Hasnain, *J. Inorg. Biochem.*, 1979, **11**, 181.
[7] C. D. Garner, L. H. Hill, N. C. Howlader, M. R. Hyde, F. E. Mabbs, and V. I. Routledge, *J. Less-Common Metals*, 1977, **54**, 270.
[8] C. D. Garner, P. Lambert, F. E. Mabbs, and T. J. King, *J.C.S. Dalton*, 1977, 1191.
[9] C. D. Garner, L. H. Hill, F. E. Mabbs, D. L. McFadden, and A. T. McPhail, *J.C.S. Dalton*, 1977, 1202.
[10] C. D. Garner, H. C. Howlader, F. E. Mabbs, P. M. Boorman, and T. J. King, *J.C.S. Dalton*, 1978, 1350.
[11] C. D. Garner, N. C. Howlader, F. E. Mabbs, A. T. McPhail, R. W. Miller, and K. D. Onan, *J.C.S. Dalton*, 1978, 1582.
[12] C. D. Garner, N. C. Howlader, F. E. Mabbs, A. T. McPhail, and K. D. Onan, *J.C.S. Dalton*, 1978, 1848.
[13] J. C. Dewar, D. L. Kepert, C. L. Raston, D. Taylor, A. H. White, and E. N. Maslen, *J.C.S. Dalton*, 1973, 2082.
[14] A. Kopwillem, *Acta Chem. Scand.*, 1972, **26**, 2941.
[15] C. D. Garner, P. Lambert, F. E. Mabbs, and J. K. Porter, *J.C.S. Dalton*, 1972, 320.
[16] D. L. McFadden, A. T. McPhail, C. D. Garner, and F. E. Mabbs, *J.C.S. Dalton*, 1975, 263.
[17] D. S. Schonland, *Proc. Phys. Soc.*, 1959, **73**, 788.
[18] A. Lund and T. Vanngard, *J. Chem. Phys.*, 1965, **42**, 2979.
[19] K. Yamanouchi and J. H. Enemark, *Inorg. Chem.*, 1979, **18**, 1626.
[20] C. D. Garner, L. H. Hill, F. E. Mabbs, D. L. McFadden, and A. T. McPhail, *J.C.S. Dalton*, 1977, 853; L. H. Hill, Ph.D. Thesis, University of Manchester, 1977; N. C. Howlader, Ph.D. Thesis, University of Manchester, 1977.
[21] G. M. Larin, A. P. M. Solochenkin, and E. V. Semenov, *Doklady Akad. Nauk S.S.S.R.*, 1974, **214**, 1343.
[22] D. A. Cruse and M. Gerloch, *J.C.S. Dalton*, 1977, 152, 1613, 1617; M. Gerloch and I. Morgenstern-Badarau, *ibid.*, p. 1619; J. E. Davies, M. Gerloch, and D. J. Phillips, *ibid.*, 1979, 1836 and refs. therein.
[23] M. Gerloch and R. C. Slade, 'Ligand-field Parameters,' Cambridge University Press, 1973.
[24] A. Abragam and H. M. L. Pryce, *Proc. Roy. Soc.*, 1951, **A205**, 135.
[25] P. D. W. Boyd, J. E. Davies, and M. Gerloch, *Proc. Roy. Soc.*, 1978, **A360**, 191; M. Gerloch and J. H. Harding, *ibid.*, p. 211.
[26] T. M. Dunn, *Trans. Faraday Soc.*, 1961, **57**, 1441.
[27] L. H. Hill, N. C. Howlader, F. E. Mabbs, M. B. Hursthouse, and K. M. Abdul Malik, *J.C.S. Dalton*, 1980, 1475.
[28] J. T. C. van Kemenade, Doctoral Thesis, Technische Hogeschool, Delft, 1970.
[29] B. R. McGarvey, *Transition Metal Chem.*, 1966, **3**, 150.
[30] B. A. Goodman and J. B. Raynor, *Adv. Inorg. Chem. Radiochem.*, 1970, **13**, 135.